

Image reconstruction and compressive sensing in MIMO radar

Bing Sun^a, Juan Lopez^b and Zhijun Qiao^c

^aSchool of Electronics and Information Engineering, Beihang University, 37 Xueyuan Road, Haidian District, Beijing 100191, China;

^bDepartment of Mathematics, University of Houston, 4800 Calhoun Road, Houston, TX 77004, USA;

^cDepartment of Mathematics, University of Texas-Pan American, 1201 West University Drive, TX 78539, USA

ABSTRACT

Multiple-input multiple-output (MIMO) radar utilizes the flexible configuration of transmitting and receiving antennas to construct images of target scenes. Because of the target scenes' sparsity, the compressive sensing (CS) technique can be used to realize a feasible reconstruction of the target scenes from undersampling data. This paper presents the signal model of MIMO radar and derive the corresponding CS measurement matrix, which shows success of the CS technique. Also the basis pursuit method and total-variation minimization method are adopted for different scenes' recovery. Numerical simulations are provided to illustrate the validity of reconstruction for one dimensional and two dimensional scenes.

Keywords: Multiple-input multiple-output, compressive sensing, basis pursuit, total-variation minimization.

1. INTRODUCTION

Multiple-input multiple-output (MIMO) radar has been a very popular topic in the last ten years since the concept was proposed in 2004,¹ which can flexibly utilize multiple transmitting and receiving antennas. The improvements of target detection and parameter identifiability make a MIMO radar more and more popular and recognized. As we know, the concept of MIMO radar is from the wireless communication field, where MIMO was developed with an amazing success. However, there still exist many challenges in the signal processing of MIMO radar. When the electromagnetic wave is irradiated to the target scene, each echo of the reflectors corresponds to one path, which therefore results in a large number of paths. Mathematically, the reconstruction of the target scene needs lot of transmitting or receiving antennas and enough sampling data, which will greatly reduce advantages of the MIMO technology.

Fortunately, the novel compressive sensing (CS) theory² can realize accurate reconstruction under the traditional Nyquist sampling rate for some sparse signals. Recently, the combination of MIMO and CS theory arises a promising research direction.³⁻⁷ The signal model of MIMO radar is a basis of synthetic aperture radar (SAR) imaging, and the CS matrix is the key of SAR image reconstruction with the compressive sensing. This paper will analyze a general signal model of MIMO radar and its image reconstruction with CS.

The whole paper is organized as follows. In Section 2 we present a signal model of MIMO radar, and then in Section 3 we derive a CS matrix by the CS theory and choose the basis pursuit method and total-variation minimization method to reconstruct the scene. In the fourth section, the simulations of one dimensional and two dimensional target scenes validate the feasibility of the CS imaging reconstruction for MIMO radar. Last section concludes the paper with some comments.

Further author information: (Send correspondence to Zhijun Qiao.)
Zhijun Qiao, E-mail: qiao@utpa.edu.

2. MIMO SIGNAL MODEL

Figure 1 shows a geometry schematic diagram with N_t transmitting antennas and N_r receiving antennas, which can be equipped flexibly. Also each of the transmitting antennas can emit different signals separately. As an imaging radar, there are N_p targets reflecting signals from the transmitting antennas to the receiving antennas. If the baseband signal of the ℓ th transmitting antenna is $x_\ell(t)$, then the radio frequency signal with carrier

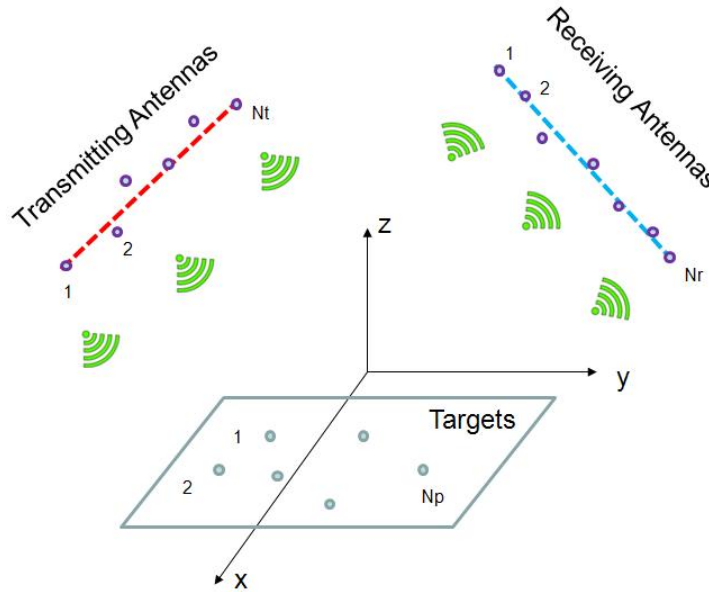


Figure 1: Geometry schematic diagram of MIMO radar.

frequency $f_{0\ell}$ is

$$s_\ell(t) = e^{2\pi i f_{0\ell} t} x_\ell(t). \quad (1)$$

Due to the demand of demodulations for different receivers, the carrier frequencies of all transmitters and receivers are required same, namely, all frequencies equal to f_0 . Let $y_m(t)$ denote the received data of the m th receiving antenna at time t , which is the superposition of the attenuated transmitting signals with time delay reflected by N_p targets with coefficients $\sigma_k, k \in [1, N_p]$. Then the received data $y_m(t)$ can be calculated through the following formula⁸

$$y_m(t) = \sum_{k=1}^{N_p} \sum_{\ell=1}^{N_t} \sigma_k e^{-2\pi i f_0 \tau_\ell^k} e^{-2\pi i f_0 \tilde{\tau}_m^k} x_\ell(t - \tau_\ell^k - \tilde{\tau}_m^k), \quad m = 1, 2, \dots, N_r \quad (2)$$

where $\tau_\ell^k = \frac{|Z_\ell^T - Z_k|}{c_0}$, $\tilde{\tau}_m^k = \frac{|Z_m^R - Z_k|}{c_0}$, and Z_ℓ^T, Z_m^R, Z_k stand for the locations of the ℓ th transmit antenna, the m th receiving antennas, and the k th target, respectively, and c_0 is the speed of light. Because $\tau_\ell^k, \tilde{\tau}_m^k$ are small and the baseband signal $x_\ell(t)$ is slowly varying usually, we may apply some approximations in (2) to get

$$y_m(t) \approx \sum_{k=1}^{N_p} \sum_{\ell=1}^{N_t} \beta_k e^{-2\pi i f_0 \tau_\ell^k} e^{-2\pi i f_0 \tilde{\tau}_m^k} x_\ell(t - t_0). \quad (3)$$

where t_0 is the time delay along with the path from the equivalent center of transmitting antennas to the equivalent center of the scene, and then to the equivalent center of receiving antennas.

Let

$$\mathbf{x}(t) = [x_1(t), \dots, x_{N_t}(t)]^T \in \mathbf{C}^{N_t \times 1}, \quad (4)$$

$$\mathbf{a}_k = \left(e^{2\pi i f_0 \tau_1^k}, \dots, e^{2\pi i f_0 \tau_{N_t}^k} \right)^T \in \mathbf{C}^{N_t \times 1}, \quad k = 1, \dots, N_p, \quad (5)$$

$$\mathbf{b}_k = \left(e^{2\pi i f_0 \bar{\tau}_1^k}, \dots, e^{2\pi i f_0 \bar{\tau}_{N_r}^k} \right)^T \in \mathbf{C}^{N_r \times 1}, \quad k = 1, \dots, N_p. \quad (6)$$

Then, the total data received at time t has the following form^{8,9}

$$\mathbf{y}(t) = \sum_{k=1}^{N_p} \sigma_k \bar{\mathbf{b}}_k \mathbf{a}_k^* \mathbf{x}(t) \quad (7)$$

where $\mathbf{y}(t) = [y_1(t), y_2(t), \dots, y_{N_r}(t)]^T \in \mathbf{C}^{N_r \times 1}$, $(\bar{\cdot})$ denotes the conjugation and $(\cdot)^*$ represents the conjugate transpose. Let us write the entire data over all time samples $\{t_1, \dots, t_N\}$ in the matrix form

$$\mathbf{y} = [\mathbf{y}(t_1) | \mathbf{y}(t_2) | \dots | \mathbf{y}(t_N)] \in \mathbf{C}^{N_r \times N}. \quad (8)$$

Then

$$\mathbf{y} = \bar{\mathbf{b}}_k \Sigma \mathbf{a}_k^* \mathbf{X}, \quad (9)$$

where

$$\Sigma = \begin{pmatrix} \sigma_1 & 0 & 0 & \dots & 0 \\ 0 & \sigma_2 & 0 & \dots & 0 \\ 0 & 0 & \sigma_3 & \dots & 0 \\ \vdots & \vdots & \vdots & \ddots & \vdots \\ 0 & 0 & 0 & \dots & \sigma_k \end{pmatrix} \quad (10)$$

and

$$\mathbf{X} = [\mathbf{x}(t_1) | \mathbf{x}(t_2) | \dots | \mathbf{x}(t_N)] \in \mathbf{C}^{N_t \times N}. \quad (11)$$

So, we get the model of MIMO signal in matrix form.

3. CS PROCESSING FOR MIMO SIGNALS

3.1 Brief introduction of CS

Based on the CS theory, if signal $\mathbf{x} \in \mathbf{C}^{N \times 1}$ is sparse in some domain, there are an orthogonal basis matrix $\Psi \in \mathbf{C}^{N \times N}$ and a coefficient vector $\mathbf{s} \in \mathbf{C}^{N \times 1}$ satisfying

$$\mathbf{x} = \Psi \mathbf{s} \quad (12)$$

where the transform coefficient \mathbf{s} can be calculated through $\mathbf{s} = \Psi^{-1} \mathbf{x}$ mathematically. If there are only $K (\ll N)$ non-zero values in \mathbf{s} , the signal \mathbf{x} is sparse in the corresponding domain, and can be reconstructed by a few random samples with very high probability. Suppose the linear observing process is $\Phi \in \mathbf{C}^{M \times N}$, where $M < N$, the observation data $\mathbf{y} \in \mathbf{C}^M$ is

$$\mathbf{y} = \Phi \mathbf{x} = \Phi \Psi \mathbf{s} = \Theta \mathbf{s} \quad (13)$$

where $\Theta = \Phi \Psi \in \mathbf{C}^{M \times N}$ is the observing matrix. The spirit of CS theory is the reconstruction of the sparse coefficient \mathbf{s} via the following optimization problem

$$\hat{\mathbf{s}} = \arg \min \|\mathbf{s}\|_0 \quad s.t. \quad \mathbf{y} = \Theta \mathbf{s}. \quad (14)$$

Because l_0 normalization optimization problem is difficult to resolve, l_0 normalization is usually replaced by l_1 normalization for the actual situation. The signal \mathbf{x} may be estimated by $\hat{\mathbf{x}} = \Psi \hat{\mathbf{s}}$. In this paper, we choose the basis pursuit (BP)^{10,11} and total variation minimization¹² (TV-min) methods to solve the above optimization problem.

The BP optimization problem is described below

$$\hat{\mathbf{s}}_{BP} = \arg \min \|\mathbf{s}\|_1 \quad s.t. \quad \mathbf{y} = \Theta \mathbf{s} \quad (15)$$

and in the case of noisy data, we solve it through adopting the method of basis pursuit denoising (BPDN)¹³

$$\hat{\mathbf{s}}_{BPDN} = \arg \min \|\mathbf{s}\|_1 \quad \text{s.t.} \quad \|\Theta\mathbf{s} - \mathbf{y}\|_2 \leq \epsilon \quad (16)$$

where $\epsilon > 0$ is a user parameter and $\|\cdot\|_2$ is the ℓ^2 norm.

Sometime, when the sparsity of \mathbf{s} is worse than its gradient, the TV-min method would be used to solve equation (14). For example, a distributed target has many non-zero reflectors, but much less non-zeros exist in the gradient image. Therefore, the above optimization problem becomes

$$\hat{\mathbf{s}}_{TV} = \arg \min \|\mathbf{s}\|_{TV} \quad \text{s.t.} \quad \mathbf{y} = \Theta\mathbf{s} \quad (17)$$

where

$$\|\mathbf{s}\|_{TV} = \sum_{i,j} \sqrt{|\mathbf{s}_{i+1,j} - \mathbf{s}_{i,j}|^2 + |\mathbf{s}_{i,j+1} - \mathbf{s}_{i,j}|^2}. \quad (18)$$

3.2 Compressive sensing matrix

From the above subsection, we can see that the CS matrix Θ plays a key rule in applying the CS to reconstruct SAR images. However, the CS matrix can not be directly extracted from the form of (9). We will rewrite (9) as an equivalently linear system to apply for other signal processing techniques.

Let \mathbf{y}_m be the total data collected at receiver m , then

$$\mathbf{y}_m = [y_m(t_1), y_m(t_2), \dots, y_m(t_N)]^T \in \mathbf{C}^{N \times 1}, \quad m = 1, 2, \dots, N_r \quad (19)$$

and for each m , define $\Theta_m \in \mathbf{C}^{N \times N_p}$ as

$$\Theta_m = \left(e^{-2\pi i f_0 \bar{\tau}_m^1} \mathbf{X}^T \bar{\mathbf{a}}_k, e^{-2\pi i f_0 \bar{\tau}_m^2} \mathbf{X}^T \bar{\mathbf{a}}_k, \dots, e^{-2\pi i f_0 \bar{\tau}_m^{N_k}} \mathbf{X}^T \bar{\mathbf{a}}_k \right), \quad m = 1, 2, \dots, N_r. \quad (20)$$

Then

$$\mathbf{y}_m = \Theta_m \Sigma^* \quad (21)$$

where $\Sigma^* = (\sigma_1, \sigma_2, \dots, \sigma_{N_p})^T \in \mathbf{C}^{N_p \times 1}$ is the scene vector. Stacking the $\mathbf{y}_m, \Theta_m, m \in [1, N_r]$ yields the following linear system⁸

$$\mathbf{Y} = \Theta \Sigma^* \quad (22)$$

where

$$\mathbf{Y} = \begin{pmatrix} \mathbf{y}_1 \\ \mathbf{y}_2 \\ \vdots \\ \mathbf{y}_{N_r} \end{pmatrix} \in \mathbf{C}^{N_r N \times 1} \quad (23)$$

and

$$\Theta = \begin{pmatrix} \Theta_1 \\ \Theta_2 \\ \vdots \\ \Theta_{N_r} \end{pmatrix} \in \mathbf{C}^{N_r N \times N_p} \quad (24)$$

Let us now substitute the above Θ into (15) or (17) to recover the targets' reflectivity coefficients through sparse treatment. For a two dimensional scene, we may scan or decompose the scene into one dimensional vectors. For example, if the pixel size of a scene is $1,000 \times 1,000$ while there are 100 non-zero reflectivity targets, we may scan the scene along with range direction (or cross range direction) pixel by pixel, then we can get a 1,000,000 point column vector with keeping the number of the non-zero reflectivity points still 100. Thus, we have $\Sigma^* = (\sigma_1, \sigma_2, \dots, \sigma_{1,000,000})^T$, and there are only 100 non-zeros values. If there are only a few points in the scene, the sparsity of the signal \mathbf{s} is obvious, while there are some distributed targets with piecewise constant reflectivity, the sparsity of the two-dimensional gradient of \mathbf{s} is better than that of itself. So, we suggest to reconstruct different scenes with different methods.

4. EXPERIMENTS

To validate the MIMO signal model and the CS reconstruction method. Three simulations are given, including 1 one-dimensional targets scene and 2 two-dimensional scenes with some random distrusted targets. The carrier frequency f_0 is 3GHz. The number of transmitters N_t is 8, and the number of samples N is 10. For our convenience, the transmitting and receiving antennas were distributed linearly along a line through the line $[x_T, -1000, 100]$ and $[x_R, 1000, 100]$, respectively, where $x_T \in [-100, 100]$ and $x_R \in [-100, 100]$.

4.1 One-dimensional simulation

The y coordinates of the one dimensional scene range from -500m to 500m at 2m increments, and the x coordinates are always 500m. We simulate 10 random points, whose reflectivity coefficients are 1 and those of the other 491 points are 0. Suppose the number of receivers $N_r = 16$, the dimension of the receiving data and the scene is 160 and 501, respectively. Obviously, this is under-determined problem. The traditional least square method cannot solve it correctly. By the consideration of the sparsity of points, the BP and TV-min methods can be used to recover the points, shown in Figure 2.

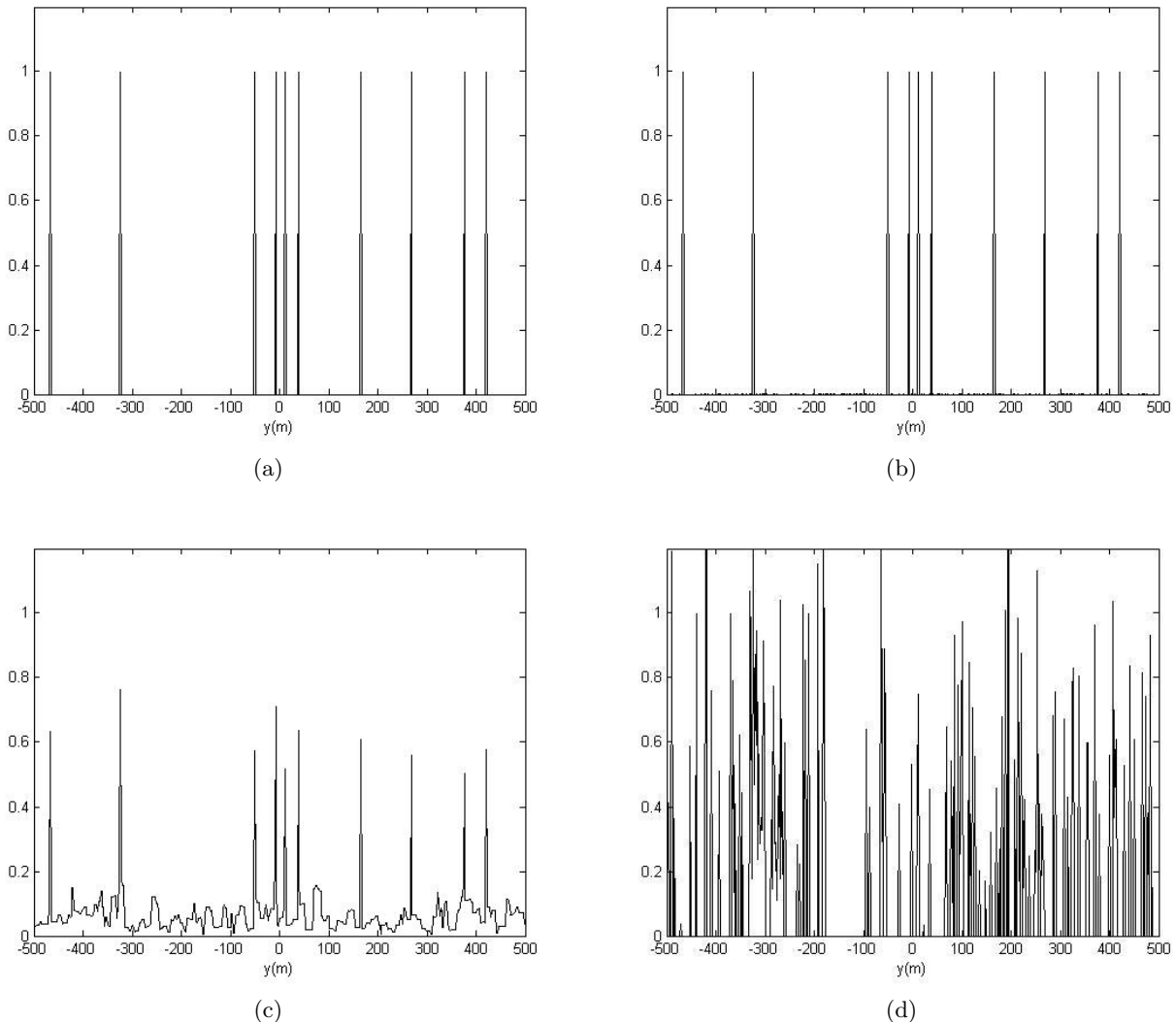


Figure 2: Simulation results of one-dimensional targets: (a) Origin random scene; (b) Recovery result by basics pursuit method; (c) Recovery result by TV-min method; (d) Recovery result by least square method.

According to the recovery results in Figure 2, the CS can be applied to a MIMO radar.

4.2 Two-dimensional simulations

Usually, imaging radar should display two dimensional scenes. In this subsection, two experiments for two-dimensional scenes are given. The x-axis range is $[400, 600]$ m, and the y-axis range is $[-100, 100]$ m. The pixel size is $2m \times 2m$.

Firstly, we simulate 10 non-zero points with random distributed in the two-dimensional scene. Figure 3 illustrates the original scene and the recovery results with the BP method, and TV-min method. According to the results, we can see that the BP method is better than the TV-min method to reconstruct a MIMO radar image.

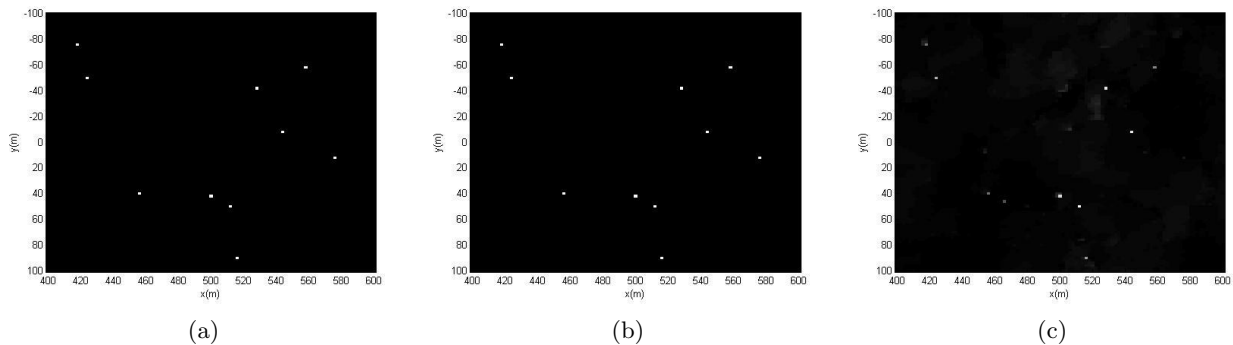


Figure 3: Simulation results of two-dimensional point target scene: (a) Origin random scene; (b) Recovery result by basics pursuit method; (c) Recovery result by TV-min method.

Furthermore, we design a scene with 3 distributed targets randomly, shown in Figure 4. Each distributed target has 10×20 non-zero points.

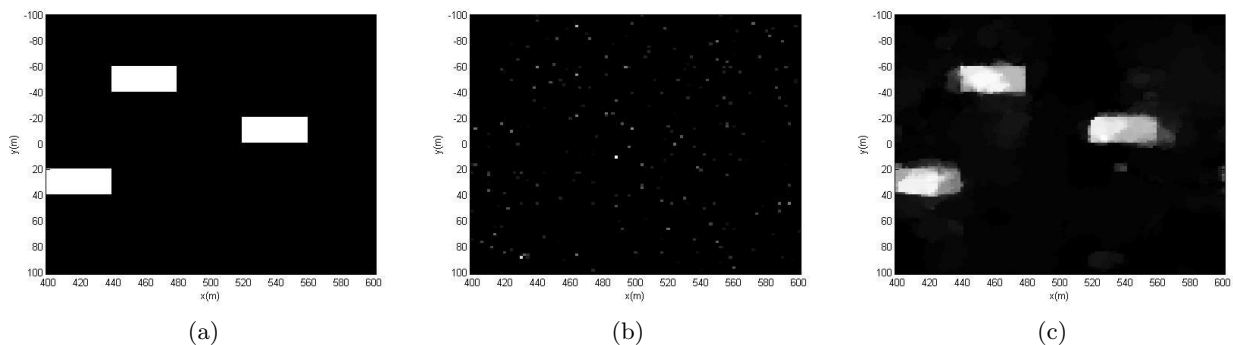


Figure 4: Simulation results of two-dimensional distributed targets scene: (a) Origin random scene; (b) Recovery result by basics pursuit method; (c) Recovery result by TV-min method.

Obviously, the result of TV-min method is much better than that of the other. It can be explained that there are totally 600 nonzero points in this scene while the dimension of the received data is only 160, so the BP method can not recover the right points directly. However, the sparsity of the scene in gradient space is much better than that in time space. So, the TV-min method will get better recovery and be more suitable for piecewise constant scenes.

5. CONCLUSION

This paper discusses the signal model of MIMO radar. For sparse targets or scenes, the CS method can be used to reconstruct the observed objects. The observing matrix and reconstruct method are also analyzed in this paper. The simulations including one-dimensional and two-dimensional results are validated for the proposed model and CS method. The BP method and TV-min method are suitable to reconstruct the sparse point scene and distributed piecewise scene, respectively.

ACKNOWLEDGMENTS

This work is supported by the National Science Fund of China (61301187 and 61328103).

REFERENCES

1. E. Fishler, A. Haimovich, R. Blum, D. Chizhik, L. Cimini, and R. Valenzuela, "Mimo radar: an idea whose time has come," in *Radar Conference, 2004. Proceedings of the IEEE*, pp. 71–78, IEEE, 2004.
2. E. J. Candès, J. Romberg, and T. Tao, "Robust uncertainty principles: Exact signal reconstruction from highly incomplete frequency information," *Information Theory, IEEE Transactions on* **52**(2), pp. 489–509, 2006.
3. C.-Y. Chen and P. Vaidyanathan, "Compressed sensing in mimo radar," in *Signals, Systems and Computers, 2008 42nd Asilomar Conference on*, pp. 41–44, IEEE, 2008.
4. Y. Yu, A. P. Petropulu, and H. V. Poor, "Compressive sensing for mimo radar," in *Acoustics, Speech and Signal Processing, 2009. ICASSP 2009. IEEE International Conference on*, pp. 3017–3020, IEEE, 2009.
5. Y. Yu, A. P. Petropulu, and H. V. Poor, "Mimo radar using compressive sampling," *Selected Topics in Signal Processing, IEEE Journal of* **4**(1), pp. 146–163, 2010.
6. Y. Yu, A. P. Petropulu, and H. V. Poor, "Measurement matrix design for compressive sensing-based mimo radar," *Signal Processing, IEEE Transactions on* **59**(11), pp. 5338–5352, 2011.
7. J. Lopez and Z. Qiao, "Array geometries, signal type, and sampling conditions for the application of compressed sensing in mimo radar," in *SPIE Defense, Security, and Sensing*, pp. 871702–1–871702–8, International Society for Optics and Photonics, 2013.
8. J. F. Lopez Jr, *Compressed sensing for multiple input-multiple output radar imaging*, THE UNIVERSITY OF TEXAS-PAN AMERICAN, 2013.
9. J. Li and P. Stoica, "Mimo radar signal processing," 2009.
10. S. Chen and D. Donoho, "Basis pursuit," in *Signals, Systems and Computers, 1994. 1994 Conference Record of the Twenty-Eighth Asilomar Conference on*, **1**, pp. 41–44, IEEE, 1994.
11. S. S. Chen, D. L. Donoho, and M. A. Saunders, "Atomic decomposition by basis pursuit," *SIAM journal on scientific computing* **20**(1), pp. 33–61, 1998.
12. A. Chambolle, "An algorithm for total variation minimization and applications," *Journal of Mathematical imaging and vision* **20**(1-2), pp. 89–97, 2004.
13. W. Lu and N. Vaswani, "Modified basis pursuit denoising (modified-bpdn) for noisy compressive sensing with partially known support," in *Acoustics Speech and Signal Processing (ICASSP), 2010 IEEE International Conference on*, pp. 3926–3929, IEEE, 2010.